Nicotiana Tabacum Tolerance to CPSMV Involves Increased H_2O_2/phenol Contents and Adjustments of Defense Protein Biosynthesis and Expression of Initiation/elongation Factors

Raissa Bret
Universidade Federal do Ceara - Campus do Pici
Yugo Lima-Melo
Universidade Federal do Ceara - Campus do Pici
Cristina Carvalho
Universidade Federal do Ceara - Campus do Pici
Jose Tadeu Abreu Oliveira (jtaolive@gmail.com.br)
Universidade Federal do Ceara - Campus do Pici https://orcid.org/0000-0003-1207-1140

Research Article

Keywords: Tobacco, CPSMV, plant defense, H2O2, phenol, PR- proteins, translation factors

Posted Date: March 17th, 2022

DOI: https://doi.org/10.21203/rs.3.rs-1428732/v1

Abstract

CPSMV is one of the various pathogens that infect cowpea (*Vigna unguiculata* L. Walp.), an important leguminous crop, and cause significant yield losses. To the best of our knowledge, there is no report on the reaction of tobacco, a model, non-leguminous plant, in response to CPSMV. In this study, we inoculated *Nicotiana tabacum* L. (var. Xanthi) leaves with a CPSMV isolate to evaluate which type of relationship (compatible, incompatible or tolerance) is established in this pathosystem and what are the plant biochemical responses to the CPSMV challenge. Tobacco plants were grown *in vitro* under controlled conditions and their leaves inoculated with CPSMV. The disease symptoms, the presence of the virus, and the tobacco biochemical responses were assessed in comparison with the mock-inoculated controls at 1, 2, and 6 days after inoculation (DAI). $CPSMV_{CE}$ modulated the activity of some enzymes and gene expression in tobacco to its own benefit, whereas, in parallel, *N. tabacum* actively responds against the viral infection. Accordingly, the severe disease symptoms caused by $CPSMV_{CE}$ in susceptible cowpea genotypes were not developed although the $CPSMV_{CE}$ viral particles were present in the tobacco leaves at 6 DAI. These findings suggest that *N. tabacum* (var. Xanthi) exhibited the patterns of a typical tolerant host to $CPSMV_{CE}$. However, a comprehensive understanding of the mechanisms of tolerance of *N. tabacum* (var. Xanthi) to $CPSMV_{CE}$ is of utmost importance to develop new cowpea genotypes tolerant or resistant to this viral disease.

Key Message

Nicotiana tabacum tolerates cowpea severe mosaic virus (CPSMV) infection by increased generation of H_2O_2 and phenol compounds and strategic adjustments of defense-related protein levels and expression of translation initiation and elongation factors.

Introduction

Cowpea severe mosaic virus (CPSMV) belongs to the family *Comoviridae*, genus *Comovirus*. The CPSMV bipartite genome is composed of two positive-sense single-stranded RNA (ssRNA), RNA 1 and RNA 2. Both RNA molecules possess a viral genome-linked protein (VPg) at the 5’ end, and a polyadenine (poly-A) tail at the 3’ end (Lomonossoff and Ghabrial, 2001). As the CPSMV genome does not have a 5’ cap, VPg functions as such by binding to the host translation factors that are hijacked to the virus advantage (Lomonossoff and Ghabrial, 2001). Viral capsid proteins exhibit several essential functions for virus infection and transmission and are usually taken as markers to detect and quantify the extent of viral infection in plants (Weber and Bujarski, 2015). The CPSMV genomic RNA 1 and RNA 2 are translated into precursor polyproteins that are processed by cysteine proteinase to generate active viral proteins (Ponz et al., 1988). This proteolytic processing can be blocked by plant proteinase inhibitors (PIN) (Gutierrez-Campos et al., 1999).

Plant viruses recruit the plant cell machinery and modulate transcript expression to infect host cells and spread systemically through the plant (Medina-Puche and Lozano-Duran, 2019). Eukaryotic translation

initiation (eIF1, eIF2, eIF3, eIF4, and eIF5) and elongation (EF-1 and EF-2) factors are host proteins indispensable for virus protein biosynthesis. Viruses use VPg to hijack these factors and produce their specific proteins (Hyodo and Okuno, 2020; Sanfaçon, 2015). The eukaryotic translation initiation factor 4E (eIF4E) and its isoform [eIF(iso)4E], as well as the eukaryotic translation elongation factor 1α (eEF1α), are the major targets of *Potyvirus* during a compatible interaction (Domier et al., 1987; Sanfaçon, 2015). Nevertheless, CPSMV is a *Comovirus* and, to our best knowledge, there is no information on eukaryotic translation factors which are used to effectively promote infection and systemic dissemination in cowpea.

In the pathosystem plant x pathogen, a compatible interaction materializes when a virus (or other pathogens) successfully infects its host, replicates, and disseminates throughout the plant. In this type of interaction, the plant cell has all factors needed for the virus replication and the plant defense is not effective or weak, resulting in disease (Garcia-Ruiz, 2019). Contrary, an incompatible interaction occurs when the plant cell does not have all or some factors needed for the virus replication and/or the plant defense armory is effective to avoid viral replication and spreading through the plant (Garcia-Ruiz, 2019). Other strategy for plant defense against virus infection lies on antiviral RNA-silencing pathways, which are pathosystem-dependent. For example, three RNA-dependent RNA polymerases (RDR1, RDR2, and RDR6) are important in the plant defense mechanisms against viruses. They participate, independently or synergistically, in the early stage of the biosynthesis of plant small interfering RNAs (siRNAs), which promote the silencing of viral RNAs in plants (Yang et al., 2011; Zhang et al., 2015a).

Upon virus infection, plants rapidly accumulate H_2O_2 that, besides to be toxic because can directly kill the pathogen, acts as an important signaling molecule. Indeed, H_2O_2 functions as a modulator of genetic reprogramming that induces several complex defense pathways (Štolfa Čamagajevac et al., 2019). For instance, increased H_2O_2 content, above the physiological levels, can lead plants to develop hypersensitive response (HR) and programmed cell death (PCD), events that are unfavorable to viruses as they are obligate biotrophic pathogens. However, despite its role in plant defense, unbalance levels of H_2O_2 content can also damage the plant tissue. To overcome such threat, plants have evolved different strategies to modulate H_2O_2 content and preserve cell redox homeostasis. The activity of enzymes such as superoxide dismutase (SOD), catalase (CAT), and ascorbate peroxidase (APX), among others, increases or decreases in response to pathogen attack, at an extent that dependent on whether the plant/pathogen pathosystem establishes a compatible or incompatible relationship (Sharma et al., 2012; Varela et al., 2017).

In addition to H_2O_2, nitric oxide (NO) also rapidly accumulated during viral infections in plants. NO, mainly produced by nitrate reductase (NR) enzyme activity, also functions as a signal molecule during viral infection to stimulate several defense responses (Štolfa Čamagajevac et al., 2019). Recently, NO generation catalyzed by NR was associated to high contents of brassinosteroids (BRs) in *Arabidopsis thaliana* challenged with Cucumber mosaic virus (CMV), which resulted in a successful antiviral defense (Zou et al., 2018).

Phenolic compounds also participate in plant defense against pathogens. They are associated with antioxidant events, activation of defense genes, cell wall reinforcement, and callose deposition (Underwood, 2012). The biosynthesis of phenol compounds and derivatives is dependent on the activity of phenylalanine ammonia-lyase (PAL) and guaiacol peroxidase (POX). PAL is the key enzyme of the phenylpropanoid pathway that is required for the biosynthesis of lignin precursors. These precursors (*p*-coumaryl, coniferyl, and sinapyl alcohols) are oxidized by POX at the expense of H_2O_2 leading to lignin accumulation and further strengthen of the cell wall (Herrero et al., 2013). The cell wall reinforcement also occurs by cross-linking of glycoproteins catalyzed by POX activity. Cell wall reinforcement reduces or prevents the spread of the virus through the plant tissue. Virus cell-to-cell movement and spreading can also be arrested when plants produce and accumulate callose inside the plasmodesmata (Harries and Ding, 2011; Walsh and Mohr, 2011). However, callose can be degraded by β-1,3-glucanase (GLU) activity. In a compatible interaction, GLU activity is induced by the virus movement protein to degrade plasmodesmata-associated callose, which facilitates virus cell-to-cell movement (Zavaliev et al., 2013).

Viruses that belong to the genus *Comovirus* infect leguminous plants, which have a high economic value worldwide. For example, susceptible cowpea genotypes can be easily infected by CPSMV (Paiva et al., 2016; Souza et al., 2017; Varela et al., 2017), which causes considerable losses in cowpea yields. Indeed, in a very recently published paper, Boari et al. (2021) reported that, under experimental (greenhouse) conditions, 39.4% and 54.3% reductions in the total number of cowpea pods and grains, respectively, and 38.9–66.2% reductions of the total weight of the grains were observed in different yardlong bean (*V. unguiculata* subsp. *sesquipedalis*) cultivars inoculated with CPSMV.

Nevertheless, to the best of our knowledge, there is no report on the reaction of tobacco, a model, non-leguminous plant, in response to CPSMV infection. A communication poster presented during the Plant Health 2019 American Physiological Society (APS) Annual Meeting, hold in Cleveland, Ohio, USA (3–7 august, 2019), described that *N. benthamiana* was systemically infected, but with an infectious CPSMV clone that had two amino acid changes in the primary structure of the CPSMV RNA1 polyprotein (Zaulda et al., 2019). Therefore, we raised the following questions: (1) why, contrary to susceptible cowpea genotypes, *N. tabacum* cv. Xanthi had no visual disease symptoms when infected with CPSMV, although the virus particles accumulated in the infected tobacco leaves; (2) which type of relationship (compatible, incompatible, or tolerance) is establish between *N. tabacum* and CPSMV?; (3) does CPSMV induce specific genetic reprogramming in *N. tabacum* cv. Xanthi and what are the resulting biochemical pathways altered?

We hypothesized that *N. tabacum* (cv. Xanthi) plants tolerate CPSMV infection through modulation of defense responses to avoid the characteristic severe symptoms observed in infected susceptible cowpea genotypes. To test this hypothesis and try to address the above questions, we evaluate in *N. tabacum* leaves the kinetic of H_2O_2 and phenol generation, the activity of defense-related enzymes, and the expression of the transcripts associated to the eukaryotic translation factor genes in the course of CPSMV infection in comparison to mock-inoculated controls.

Material And Methods

2.1. Plant propagation and in vitro growth

Nodal segments of *Nicotiana tabacum* L. (var. Xanthi) previously grown under *in vitro* conditions were used for plant propagation. Two plants were grown in a 250 mL glass container (90 mm x 60 mm) sealed with a transparent polyethylene lid, containing 25 mL of the complete Murashige and Skoog (MS) basal culture medium (Murashige and Skoog, 1962), pH 5.8, enriched with 4% (m/v) sucrose and 0.7% (m/v) agar, previously autoclaved at 121°C and 1.5 x 10^5 Pa for 15 min. The growth conditions were 12 h light/12 h dark photoperiod, with photosynthetically active radiation (PAR) of 35 µmol (photons) m^{-2} s^{-1} provided by phosphorescent lamps, at 28°C, for 45 days before the onset of the experiments.

2.2. CPSMV inoculation

Inoculums of the Cowpea severe mosaic virus, $CPSMV_{CE}$ isolate (Lima et al., 2011), were prepared as previously reported (Silva et al., 2016) from leaves of a susceptible cowpea (*Vigna unguiculata* L. Walp.) genotype (CE-31, syn. Pitiuba) that exhibited the characteristic disease symptoms. The infected cowpea leaves were collected 6 days after the $CPSMV_{CE}$ inoculation and maintained at -80 ºC until use. To prepare the virus inoculums, the infected cowpea leaves were taken from the ultra-freezer, macerated in a mortar and pestle with 10 mM potassium-phosphate buffer, pH 7.0, containing 0.01% (m/v) sodium sulfite and 600-mesh carborundum powder (1:10, m/v) used as an abrasive. Tobacco plant inoculation was done by rubbing the adaxial and abaxial surface of fully expanded leaves with the $CPSMV_{CE}$ inoculum, 45 days after the initiation of the nodal segment propagation. The suspension to treat the mock-inoculated control was obtained using the same above procedure, but using virus-free, healthy cowpea leaves. Mock- or $CPSMV_{CE}$-inoculated leaves were detached with the aid of a scalpel blade at 1, 2, and 6 days after inoculation (DAI), at the junction between the petiole and the stem. These leaves were immediately frozen in liquid nitrogen and stored at -80 ºC until use.

2.3. Protein extraction and quantification

Mock- and $CPSMV_{CE}$-inoculated tobacco leaves were taken from the ultra-freezer (-80 ºC) and pulverized using a mortar and pestle in liquid nitrogen to a fine powder. This powder was mixed (1:8, m/v) with 100 mM potassium-phosphate buffer, pH 7.0, containing 150 mM NaCl, and the proteins extracted for 3 h at 4 ºC, under gentle agitation. The suspension obtained was filtered twice using cheesecloth and centrifuged (15.000 *g*, 4 ºC, 20 min). The supernatant (crude extract) was recovery and used for protein quantification and measurement of enzyme activity as described below. Quantification of the soluble leaf proteins was performed following the Bradford (1976) assay method, using bovine serum albumin (BSA) as a standard protein. Data were expressed as mg protein g^{-1} fresh matter (mg g^{-1} FM).

2.4. Enzyme activity assays

The activity assays of superoxide dismutase (SOD; EC 1.15.1.1), catalase (CAT; EC. 1.11.1.6), ascorbate peroxidase (APX; EC. 1.11.1.11), phenylalanine ammonia-lyase (PAL; EC 4.3.1.5), guaiacol peroxidase

(POX; EC 1.11.1.7), β-1,3-glucanase (GLU; EC 3.2.1.39), and papain inhibitor (PIN) were performed using the leaf crude extracts from three independent biological samples each from three technical independent replicates.

SOD activity was measured based on the photochemical reduction inhibition of nitroblue-tetrazolium (NBT) to blue formazan (van Rossum et al., 1997). The increases in absorbance at 630 nm (Automated Microplate Reader ELX800, BioTek®, Vermont, USA) were recorded every 1-min interval, for 5 min, during the exposure of the reaction mixtures to a 32 W fluorescent lamp. The absorbance measured prior to light exposure was used as the correction factor. A similar reaction mixture in which an 0.1 mL aliquot of 100 mM potassium-phosphate buffer, pH 7.0, containing 150 mM NaCl, replaced the crude extract was used as blank for each tested sample. One unit of SOD activity (1 UA) was defined as the volume of the leaf crude extract, in mL, that inhibits 50% of the NBT photochemical reduction. The specific activity of SOD was expressed in UA per milligram protein (UA mg^{-1} protein).

CAT was assayed as previously described (Havir and McHale, 1987), with minor modifications (Peixoto et al., 1999), by measuring the consumption of hydrogen peroxide (H_2O_2) from the reaction mixture based on the decrease in absorbance at 240 nm (Spectrophotometer Genesys 10S UV-Vis, ThermoScientific™, Waltham, USA), recorded every 10-s interval, for 1 min. The absorbance measured at 10 s after the onset of the reaction was used as blank for every sample. One unit of CAT activity (UA) was assumed as the decrease of one absorbance unit per mL of sample per min and was expressed as specific activity (UA mg^{-1} protein).

APX activity was assayed as previously described (Koshiba, 1993) by measuring the consumption of H_2O_2. The reaction mixture contained ascorbic acid and H_2O_2 as substrates. During the course of the reaction, the decrease in absorbance at 290 nm (Spectrophotometer Genesys 10S UV-Vis, ThermoScientific™, Waltham, USA) was recorded at every 20-s interval up to 2 min. The absorbance measured at 10 s after the onset of the reaction was used as blank. One unit of APX activity (UA) was assumed as the decrease of one absorbance unit per mL of sample per min and was expressed as specific activity (AU mg^{-1} protein)

PAL activity was assayed as described by Varela et al. (2017). The method is based on the formation of trans-cinnamic acid (TCA) by the action of PAL on L-phenylalanine used as substrate. A reactional mixture in which the substrate addition was done after stopping the reaction was used as the control for each sample. TCA was detected by absorbance readings at 290 nm (Spectrophotometer Genesys 10S UV-Vis, ThermoScientific™, Waltham, USA). PAL activity was calculated using a standard curve of known TCA concentrations. The specific activity was expressed as μmol TCA per milligram protein per min (μmol TCA mg^{-1} protein min^{-1}).

POX activity was assayed according to Urbanek et al. (1991), based on the tetraguaiacol production resulting from the electron transfer from H_2O_2 to guaiacol, by measuring the increase in absorbance at 480 nm (Spectrophotometer Genesys 10S UV-Vis, ThermoScientific™, Waltham, USA), at every 20-s

interval for 2 min. The absorbance measured at 10 s after the onset of the reaction was used as blank. One unit of POX activity (UA) was assumed as the increase of one absorbance unit per mL of sample per min and was expressed as specific activity (UA mg^{-1} protein).

GLU activity was assayed as described by Boller (1993). The method is based on the enzymatic liberation of glucose from laminarin used as substrate. Absorbance readings were taken at 520 nm (Spectrophotometer Genesys 10S UV-Vis, ThermoScientific™, Waltham, USA) and the glucose content released in the reaction mixture was calculated using a standard curve of known glucose concentrations. The reaction mixture in which the buffer replaced the sample was taken as the blank. The specific activity was expressed in nanokatal (nkat) of glucose per milligram protein (nkat mg^{-1} protein). One nkat was defined as one nmol of glucose liberated from laminarin per mL of sample per second, under the assay conditions.

Inhibition of the proteolytic activity of papain (EC 3.4.22.2), a cysteine proteinase, by the cowpea leaf crude extracts was evaluated as previously described (Abe et al., 1992) by measuring the inhibition of the enzymatic release of β-naphthylamine from N-α-benzoyl-arginine-β-naphthylamide (BANA) used as the enzyme substrate. The product of the interaction between β-naphthylamine and 4-dimethylaminocinnamaldehyde (DMACA) was measured at 540 nm. The positive control (100% papain activity) reaction was performed by adding an aliquot of the buffer solution instead of the corresponding leaf crude extract. The blank for each leaf crude extract sample consisted of the complete reaction mixture to which BANA was added after the reaction had been stopped. The level of papain inhibition was measured by the decrease in absorbance at 540 nm (Spectrophotometer Genesys 10S UV-Vis, ThermoScientific™, Waltham, USA). One unit of inhibition (UI) was defined as the decrease in 0.01 absorbance unit caused by the addition of the leaf crude extract sample in comparison to the absorbance verified in the positive control (100% papain activity) per milliliter of sample. Specific inhibitory activity was expressed as UI mg^{-1} protein.

2.5. Quantitative assay of phenolic compounds

Phenolic compounds (PC) were extracted and quantified according to Ainsworth and Gillespie (2007). Tobacco fresh leaves (500 mg) were pulverized to a fine powder using a mortar and pestle with liquid nitrogen and extracted with 1.0 mL 95% (v/v) methanol. The suspension was mixed for 3 min, centrifuged (13,000 *g*, 25 ºC, 5 min), and the supernatant was used to perform the assay, using the Folin-Ciocalteu reagent under alkaline condition. The absorbance of the mixture was taken at 765 nm (Spectrophotometer Genesys 10S UV-Vis, ThermoScientific™, Waltham, USA). The amount of PC was calculated based on a standard curve of known concentrations of pyrogallic acid. It was expressed as mg PC per gram fresh matter (mg g^{-1} FM).

2.6. Qualitative and quantitative assay of H_2O_2

The presence of H_2O_2 in tobacco leaves was performed by the *in situ* 3,3'-diaminobenzidine (DAB) staining method (Thordal-Christensen et al., 1997). The DAB solution (0.1%, m/v) was prepared by

adjusting the pH to 3.0 with HCl and solubilized in ultra-pure water at 50 ºC for 1 h. After cooling, the pH was adjusted to 4.0 with NaOH. The petiole was submerged in the DAB solution under dark conditions immediately after the leaves had been detached from the plant stem. After 8 h, the leaves were depigmented by 24h immersion in a solution of trichloroacetic acid (1.5 g L^{-1}) in ethanol and chloroform (3:1, v/v), under slight agitation. The presence of H_2O_2 was qualitatively evaluated by the presence of dark brown precipitates.

H_2O_2 extraction and quantification were performed using the Amplex® Red Hydrogen Peroxide/Peroxidase Assay Kit (Invitrogen, Carlsbad, CA, USA) according to Zhou et al., (1997). The method is based on the reaction of the Amplex Red reagent (10-acetyl-3,7-dihydrophenoxazine) and H_2O_2 (1:1 proportion) in the presence of horseradish peroxidase. The reaction was conducted in wells of 96-well microplates and absorbance readings were taken at 540 nm (Automated Microplate Reader ELX800, BioTek®, Vermont, USA). The H_2O_2 content was calculated using a standard curve of known H_2O_2 concentrations and was expressed as nanomol de H_2O_2 per gram of fresh matter (nmol H_2O_2 g^{-1} FM).

2.7. Reverse transcription-polymerase chain reaction (RT-PCR) analysis for $CPSMV_{CE}$ detection in tobacco leaves

To check for the presence or absence of $CPSMV_{CE}$ in susceptible cowpea and in non-inoculated (mock-) and virus-inoculated tobacco leaves, degenerate primers, corresponding to the specific and conserved sequence of the coat protein (CP) gene within the genus Comovirus, were used as templates: 5'-YTCRAA WCCVYTRTTKGGMCCACA-3' (reverse) and 5'-GCATGGTCCACWCAGGT-3' (forward) (Brioso et al. 1996). The RT-PCR products obtained (Martins et al., 2020) were subjected to agarose gel (1.2%, m/v) electrophoresis (100 mA constant current, 30 min, 26°C) and next the gel was immersed in ethidium bromide (0.5 µg/µL) for 10 min. Visualization of the RT-PCR products was achieved using an UV light transilluminator. Photo-documentation was done using a MiniBIS Pro Bio-Imaging Systems + GelCapture™ software.

2.8. RNA extraction from tobacco leaves and quantitative reverse transcription-polymerase chain reaction (qRT-PCR) for analysis of the relative expression levels of selected genes

Total RNA was extracted from tobacco leaves using the NucleoSpin® RNA Plant kit (Macherey-Nagel, Düren, Germany) as advised by the manufacturer. The extracted RNA was quantified (NanoDrop 2000 spectrophotometer, ThermoScientific™, Waltham, USA) and its integrity was checked after electrophoresis in 1.5% (m/v) agarose gel performed in a Pharmacia Biotec electrophoresis system, at 50 mA, 100 V. The purified RNAs were reverse transcribed to cDNAs by RT-PCR (ImProm-II™ Reverse Transcription System, Promega, Madison, USA) according to the manufacturer's instructions. Initially, the mixture containing the

RNAs, RNase-free water, and the oligo(dT)s were incubated in a thermocycler (Endurance TC-512, Techne®, Burlington, USA) at 70 ºC for 5 min, and chilling at 4 ºC for 5 min. Next, the Reverse Transcription Mix and oligo(dT)s were added and the annealing step carried out at 25 ºC for 5 min, elongation at 42 ºC for 60 min, and the enzyme denaturation at 70 ºC for 15 min. The synthesized cDNAs were kept under − 20 ºC until use. The relative levels of the mRNAs (transcripts) of the corresponding genes *RDR1* (RNA-dependent RNA polymerase 1), *RDR2* (RNA-dependent RNA polymerase 2), *EF1α* (elongation factor 1α), *eIF4E* (eukaryotic translation initiation factor 4E) and its isoform *eIF(iso)4E*, *NR* (nitrate reductase), *BRI1* (brassinosteroid insensitive 1), *BAK1* (BRI1-associated receptor kinase 1), and *RBOHB* (respiratory burst oxidase homolog protein B) was estimated using the GoTaq® qPCR Master Mix for Dye-Based Detection (Promega, Madison, USA) following the manufacturer's instructions and performed on a Mastercycler® RealPlex4 (Eppendorf, Hamburg, Germany). The schedule used for quantitative reverse transcription-polymerase chain reaction (qRT-PCR) analysis was: enzyme activation at 94 ºC for 10 min; 40 cycles of denaturation at 94 ºC for 15 s, annealing at 41.0, 56.6, 57.3, 61.0, or 62.5 ºC for 15 s, elongation at 60 ºC for 20 s; and a final elongation step at 60 ºC for 2 min. The relative quantification (relative gene expression) of transcripts was performed using the $2^{-\Delta\Delta Ct}$ method (Livak and Schmittgen, 2001). The genes *L23A1, L23A3, PP2A*, and *F-BOX*, which code for the ribosomal protein L23A1, ribosomal protein L23A1, phosphatase 2A, and F-box protein, respectively, were tested to determine the most stable reference (housekeeping) genes (Martins et al., 2020) across the biological and technical replicates to calculate the relative gene expression. *PP2A* was the most stable and thus selected as the housekeeping gene. The forward and reverse primers used for qRT-PCR analyses were designed based on the cowpea mRNA sequences available at NCBI using the Perl Primer v1.1.19 software. Primer efficiency was determined by the dilution method and efficiencies between 95 and 100% were achieved. Reaction products were analyzed by melting curves to verify the absence of unspecific products and dimer formation.

2.9. Experimental design and statistical analysis

The experiments were set in a completely randomized design in a factorial arrangement (2 treatments x 3 days of measurement), with three independent biological replicates. Each biological replicate was represented by 5 or 6 plants. Three independent analyses (technical replicates) were performed on three independent biological replicates for each studied time point. The mean of three independent biological replicates was calculated. One-way ANOVA was carried out and means were compared between CPSMV- and mock-inoculated tobacco plants within each day using the Student's T-test ($p \leq 0.05$), whereas the Tukey's test ($p \leq 0.05$) was employed to detect any difference between the means of the distinct experimental days after inoculation (1 DAI, 2 DAI, and 6 DAI) within the same treatment. Analyses were done with three technical replicates for each biological replicate.

Results

3.1. Detection of $CPSMV_{CE}$ in tobacco leaves

Tobacco leaves inoculated with $CPSMV_{CE}$ accumulated cDNA fragments of the CPSMV-coat protein at 6 DAI (Fig. 1A) to a lesser extent than the susceptible cowpea genotype (CE-31) that was used for comparison and similarly inoculated with the virus (Fig. 1A). However, contrary to cowpea, no characteristic symptoms of the viral disease or morphological changes were developed in tobacco leaves even at 30 DAI (data not shown).

3.2. Soluble protein and RNA contents in tobacco leaves

The protein contents (Fig. 1B) in the mock- and $CPSMV_{CE}$-inoculated tobacco leaves did not vary significantly within the same treatment group along the experimental period (same lowercase letter). However, comparison between the two studied plant groups showed that the protein contents of the $CPSMV_{CE}$-inoculated tobacco leaves were significantly ($p \leq 0.05$) lower (different uppercase letters) than those in the respective mock-inoculated plants at 1 DAI (2.66 ± 0.14 mg protein g^{-1} FM versus 3.72 ± 0.15 mg protein g^{-1} FM; 28% decrease) and 6 DAI (2.47 ± 0.08 mg protein g^{-1} FM versus 4.07 ± 0.06 mg protein g^{-1} FM; 39% decrease).

The RNA contents (Fig. 1C) within the mock-inoculated control group decreased significantly ($p \leq 0.05$) at 2 DAI (7.15 ± 1.16 mg RNA g^{-1} FM) and stayed lower at 6 DAI (8.14 ± 0.17 mg RNA g^{-1} FM) as compared with the value at 1 DAI (10.37 ± 0.16 mg RNA g^{-1} FM). In contrast, the RNA contents of the $CPSMV_{CE}$-inoculated tobacco leaves significantly ($p \leq 0.05$) increased from 1 DAI (4.09 ± 0.24 mg RNA g^{-1} FM) to 2 DAI (6.92 ± 0.92 mg RNA g^{-1} FM), but at 6 DAI decreased to 3.59 ± 0.69 mg RNA g^{-1} FM, a value which is not significantly different when compared to that calculated at 1 DAI. The RNA contents in the $CPSMV_{CE}$-inoculated tobacco leaves at 1 DAI (4.09 ± 0.24 mg RNA g^{-1} FM) and 6 DAI (3.59 ± 0.69 mg RNA g^{-1} FM) were significantly ($p \leq 0.05$) lower (~ 60% and 56% decrease, respectively) as compared with the corresponding data for the mock-inoculated leaves at the corresponding experimental periods (1 DAI = 10.37 ± 0.16 mg RNA g^{-1} FM; and 6 DAI = 8.14 ± 0.17 mg RNA g^{-1} FM). At 2 DAI the data found for the $CPSMV_{CE}$-inoculated tobacco leaves (6.92 ± 0.92 mg RNA g^{-1} FM) was not significantly different compared with that of the control plants (7.15 ± 1.16 mg RNA g^{-1} FM).

3.3. H_2O_2 content and SOD, CAT, and APX enzyme activities in tobacco leaves

Qualitatively, the presence of H_2O_2 in the $CPSMV_{CE}$-inoculated leaves, observed by naked eyes, barely increased in comparison to the mock-inoculated controls at 1 DAI, 2 DAI, and 6 DAI, as detected by the DAB staining method (Fig. 2A). Nevertheless, the H_2O_2 accumulation was more evident at the leaf midrib and secondary veins. However, the quantitative estimation of the H_2O_2 contents (Fig. 2B) revealed significant ($p \leq 0.05$) higher amounts in the $CPSMV_{CE}$-inoculated tobacco leaves at 1 DAI (11.87 ± 0.87 nmol H_2O_2 g^{-1} FM) (~ 40% increase) and 6 DAI (14.71 ± 0.05 nmol H_2O_2 g^{-1} FM) (~ 34% increase) in comparison with the respective mock-inoculated controls (1 DAI = 7.16 ± 1.50 nmol H_2O_2 g^{-1} FM; 2 DAI = 9.71 ± 0.54 nmol H_2O_2 g^{-1} FM). At 2 DAI, the H_2O_2 contents were similar.

The SOD specific activity data (Fig. 3A) in the $CPSMV_{CE}$-inoculated tobacco leaves markedly increased (~ 155% and 180%, respectively) at 6 DAI (3.11 ± 0.33 UA mg^{-1} protein) in comparison to those at 1 DAI (1.22 ± 0.07 UA mg^{-1} protein) and 2 DAI (1.11 ± 0.25 UA mg^{-1} protein), values that were not significantly different. The SOD specific activity data of the mock-inoculated control increased (35%) at 2 DAI (1.85 ± 0.26 UA mg^{-1} protein) in relation to 1 DAI (1.37 ± 0.07 UA mg^{-1} protein), but decreased at 6 DAI (1.52 ± 0.15 UA mg^{-1} protein) to a value that was not different from that verified at 1 DAI (1.57 ± 0.15 UA mg^{-1} protein). Nevertheless, the $CPSMV_{CE}$ challenge of tobacco induced a 68% increase in the SOD activity at 6 DAI over that of the mock plants at 2 DAI.

The CAT specific activity (Fig. 3B) of the $CPSMV_{CE}$-inoculated leaves stayed approximately similar from 1 DAI to 6 DAI (1 DAI = 0.73 ± 0.02 UA mg^{-1} protein; 2 DAI = 0.59 ± 0.16 UA mg^{-1} protein; 6 DAI = 0.59 ± 0.12 UA mg^{-1} protein), whereas that of the mock-inoculated control significantly ($p \leq 0.05$) increased from 1 DAI (1.03 ± 0.12 UA mg^{-1} protein) to 2 DAI (1.35 ± 0.05 UA mg^{-1} protein), but decreased considerably (60%) at 6 DAI (0.53 ± 0.06 UA mg^{-1} protein). In addition, besides to present similar data along the studied experimental time course, the CAT specific activity values (Fig. 3B) of the $CPSMV_{CE}$-inoculated leaves were significantly ($p \leq 0.05$) lower than those of the mock-inoculated control at 1 DAI and 2 DAI, except at 6 DAI.

The APX specific activity (Fig. 3C) of the CPSMV-inoculated leaves decreased (~ 19%) significantly ($p \leq 0.05$) at 2 DAI (6.65 ± 0.86 UA mg^{-1} protein), but increased notably (~ 48%) at 6 DAI (12.21 ± 0.67 UA mg^{-1} protein) in comparison to the data at 1 DAI (8.23 ± 0.93 UA mg^{-1} protein). In the mock-inoculated control, the APX specific activity increased significantly ($p \leq 0.05$) at 2 DAI (8.12 ± 0.37 UA mg^{-1} protein) and 6 DAI (7.23 ± 0.91 UA mg^{-1} protein) in comparison with the data at 1 DAI (5.33 ± 1.55 UA mg^{-1} protein). Comparatively, the APX specific activity values of the CPSMV-inoculated leaves were higher at 1 DAI (8.23 ± 0.93 UA mg^{-1} protein) and at 6 DAI (12.21 ± 0.67 UA mg^{-1} protein) than those respective mock-inoculated control values (1 DAI = 5.33 ± 1.55 UA mg^{-1} protein; 6 DAI = 7.23 ± 0.91 UA mg^{-1} protein). At 2 DAI, the data did not differ significantly (mock-inoculated = 8.12 ± 0.37 UA mg^{-1} protein; CPSMV-inoculated = 6.65 ± 0.86).

3.4. Phenolic compound content and PAL and POX enzyme activities in tobacco leaves

The contents of phenolic compounds (PC) (Fig. 4A) in the $CPSMV_{CE}$-inoculated tobacco leaves was significantly higher at 1 DAI (7.19 ± 0.75 mg PC g^{-1} FW) and 6 DAI (15.37 ± 1.21 mg PC g^{-1} FW) in comparison with the corresponding mock-inoculated controls (1 DAI = 4.28 ± 0.47 mg PC g^{-1} FW; 6 DAI = 11.15 ± 1.10 mg PC g^{-1} FW).

In parallel, the PAL activity (Fig. 4B) was significantly higher in $CPSMV_{CE}$-inoculated leaves at 1 DAI (1.28 ± 0.07 µmol TCA mg^{-1} protein min^{-1}), 2 DAI (2.08 ± 0.09 µmol TCA mg^{-1} protein min^{-1}), and 6 DAI (2.22

± 0.00 µmol TCA mg^{-1} protein min^{-1}) in comparison with the respective mock-inoculated controls (1 DAI = 0.48 ± 0.06 µmol TCA mg^{-1} protein min^{-1}; 2 DAI = 1.08 ± 0.13 µmol TCA mg^{-1} protein min^{-1}; 6 DAI = 0.78 ± 0.19 µmol TCA mg^{-1} protein min^{-1}).

The POX activity (Fig. 4C) was similar between the $CPSMV_{CE}$- and mock-inoculated at 1 DAI and 2 DAI. However, the tobacco leaves responded to the CPSMV challenge with a very prominent increase (~ 3x) at 6 DAI (120.80 ± 5.38 UA mg^{-1} protein) in relation to the mock-inoculated (control) control (38.58 ± 3.79 UA mg^{-1} protein).

3.5. Enzyme activities of the PR-proteins GLU and PIN in tobacco leaves

The GLU activity (Fig. 5A) in CPSMV-inoculated tobacco leaves (1.85 ± 0.07 nkat mg^{-1} protein) was not different from the data calculated for the mock-inoculated control (1.73 ± 0.23 nkat mg^{-1} protein) at 1 DAI, neither at 2 DAI (2.50 ± 0.31 nkat mg^{-1} protein and 1.92 ± 0.12 nkat mg^{-1} protein, respectively). However, the GLU activity in CPSMV-inoculated tobacco leaves (2.65 ± 0.16 nkat mg^{-1} protein) more than doubled in relation to that calculated for the mock-inoculated control at 6 DAI (1.02 ± 0.11 nkat mg^{-1} protein).

The protease inhibitor (PIN) activity (Fig. 5B) was significantly higher at 1 DAI (455.35 ± 17.81 UI mg^{-1} protein) and 2 DAI (361.46 ± 27.95 UI mg^{-1} protein) when compared with the respective mock-inoculated controls (1 DAI = 211.10 ± 19.52 UI mg^{-1} protein; 2 DAI = 299.19 ± 14.04 UI mg^{-1} protein), even taken into consideration that controls presented a crescent trend of PIN activity along the time course.

3.6. Relative expression of the selected transcripts

Challenge of the tobacco leaves with $CPSMV_{CE}$ up-regulated (1.45-fold change) the relative expression of the *eIF4E* gene in comparison with the mock-inoculated control, at 6 DAI (Fig. 6). *RDR2* gene slightly increased but not significantly. By contrast, significant decreases in the relative levels of the following transcripts were detected in the $CPSMV_{CE}$-inoculated leaves in comparison with the mock-inoculated control (Fig. 6): *EF1α* (0.45-fold); *NR* (0.64-fold); and *BRI1* (0.46-fold). No significant changes were noted for *RDR1*, *eIF(iso)4E*, *RBOHB*, and *BAK1*.

Discussion

Effective infection of tobacco and cowpea leaves by $CPSMV_{CE}$ was detected based on the presence of the corresponding cDNA fragments of the CPSMV-coat protein (Fig. 1A). Somehow, tobacco accumulated less viral particles than the susceptible cowpea genotype. Severe mosaic and chlorosis, which are typical symptoms observed in the virus-susceptible cowpea genotype CE-31 inoculated with $CPSMV_{CE}$, were not noticed in the tobacco leaves (Fig. 1B), even at 30 days after inoculation (figure not shown). $CPSMV_{CE}$ accumulation was previously reported in CE-31 (Souza et al., 2017; Varela et al., 2017), which

characterize a compatible interaction. This suggests that the studied tobacco variety (Xanthi) is tolerant to $CPSMV_{CE}$, as it limits the virus disease severity and established a style of asymptomatic co-existence (Sanfaçon, 2020) probably through induction of specific mechanisms, most of them still not well understood because tolerance, in comparison with resistance to plant pathogens, has received much less attention. Consequently, experimental results and data on the mechanism of tolerance that helps plants to prevent the severe symptoms observed in susceptible hosts are scarce in the pertinent literature (Pagán and Garcia-Arenal, 2018). Nevertheless, in tolerant interactions, considerable accumulation of viruses has been observed in asymptomatic plants (Sanfaçon, 2020). Then, what biochemical responses are induced by $CPSMV_{CE}$ in tobacco (var. Xanthi) plants to attain tolerance is an open question. To address this demand, we challenged tobacco plants with $CPSMV_{CE}$ and compared with mock-inoculated controls.

Lower accumulation of soluble proteins and RNA in $CPSMV_{CE}$-inoculated tobacco leaves (Fig. 1B, C) might be a plant strategy to reduce the available cellular machinery for virus replication. Lower protein and RNA contents is a broadly-known plant response against virus infection in consequence of gene silencing and protein target to degradation (Garcia-Ruiz, 2018; Souza et al., 2017). Protein degradation and the resulting constituent amino acids are linked to the supply of energy and metabolic intermediates necessary for an effective defense strategy (Rojas et al., 2014). Recently, a proteomic study carried out by our research group showed that proteins involved in RNA metabolism, in addition to specific transcription factors, were less accumulated in resistant cowpea plants inoculated with $CPSMV_{CE}$ (Varela et al., 2017).

Part of the defense mechanism of tobacco plants against $CPSMV_{CE}$ infection consisted of increased H_2O_2 content at 1 and 6 DAI (Fig. 2). H_2O_2 accumulation in tobacco leaves is similar to that in cowpea, either in susceptible or resistant genotypes (Paiva et al., 2016; Silva et al., 2016; Souza et al., 2017), possibly as an attempt to limit the $CPSMV_{CE}$ spread in the host plants at the earlier stages of infection. At this infection phase, H_2O_2 accumulation may act as a microbicidal agent at the site of pathogen invasion and also as a signaling molecule to trigger the plant defense responses (Deng et al., 2016; Lei et al., 2016; Zhang et al., 2020).

One of the sources of H_2O_2 production in plants is dismutation of superoxide anions ($O_2^{\bullet -}$) catalysed by SOD (Smirnoff and Arnaud, 2019). The SOD activity of the $CPSMV_{CE}$-inoculated tobacco plants (Fig. 3A) increased remarkably (180%) at 6 DAI in comparison to the respective mock-inoculated control. Changes in SOD activity and H_2O_2 content in $CPSMV_{CE}$-inoculated tobacco plants apparently did not match, apart from 6 DAI when both SOD and H_2O_2 increased concomitantly. However, the net amount of H_2O_2 is also dependent on CAT, APX, and POX activities as they use H_2O_2 as substrate and thus are scavenge enzymes. As shown in Fig. 3B, 3C, and 4C, whereas CAT activity is overall lower, APX and POX are much higher, particularly at 6 DAI, in comparison to the respective tobacco plant controls. Together, these data would suggest that H_2O_2 should be lower at 6 DAI. However, SOD is regarded as the main intracellular antioxidant defense against superoxide anions, which are converted into H_2O_2 and O_2 (Stephenie et al., 2020), and may have overwhelmed APX and POX activities to explain the net high amount of H_2O_2 at 6

DAI. Moreover, there are other many biochemical ways, non- and enzymatic, by which H_2O_2 is produced in plants such as mitochondrial generation through the electron transport chain (ETC), oxidases involved in photorespiration, photosynthesis, fatty acid oxidation, amine/polyamine oxidation, and purine catabolism (Smirnoff and Arnaud, 2019). As previously mentioned, H_2O_2 accumulation may act as a direct toxic agent against $CPSMV_{CE}$ at the site of pathogen invasion. For instance, H_2O_2 was considered an effective agent for *in vitro* inactivation of adenovirus types 3 and 6, adenoassociated virus type 4, rhinoviruses 1A, 1B, and type 7, myxoviruses, influenza A and B, respiratory syncytial virus, and coronavirus strain 229E (Mentel et al., 1977). In addition of being antimicrobial, H_2O_2 acts as a signalling molecule in the induction of systemic acquired resistance (SAR) and defence-associated genes in plants (Smirnoff and Arnaud, 2019). Lei and collaborators (2016) showed that the M strain of Cucumber mosaic virus (M-CMV) induced H_2O_2 accumulation in inoculated leaves of *Nicotiana tabacum* (cv. white burley) during systemic infection, compared with mock-inoculated leaves. Previous works suggested that the higher activities of SOD, APX, and POX, and the lower activity of CAT, compared to mock-inoculated controls, were associated to plant defense mechanisms against virus infection (Gonçalves et al., 2013; Souza et al., 2017; Varela et al., 2017).

In our study, the phenolic compound content increased at 1 DAI and 6 DAI (Fig. 4A) and the PAL activity was considerably higher at all studied time points (Fig. 4B) in $CPSMV_{CE}$-inoculated tobacco leaves, compared with the respective mock-inoculated controls. Therefore, both the increased PAL activity and the biosynthesis of secondary compounds (phenols) appeared to be important in conferring tolerance of tobacco plants to $CPSMV_{CE}$. In most plants, the key step of the biosynthesis of phenolics is the non-oxidative deamination of phenylalanine by PAL to *trans*-cinnamate, which constitutes the initial reaction of the phenylpropanoid pathway. In wheat plants infected with Wheat streak mosaic virus the phenylpropanoid pathway was stimulated upon infection, but lignification was not (Kofalvi and Nassuth, 1995). When the cotyledons of 3–true leaf potted seedlings of a common Japanese tomato cultivar (cv. Fukuju No. 2) were inoculated with potato Virus X (PVX) and with an attenuated strain (L11A) of tobacco mosaic virus (TMV-L11A), the time-course analysis of the methanol-extractable free, and saponifiable ester-bound phenol contents accumulated significantly in the primary leaves during the first 3 days, continued to increase steadily, and peaked between 6 and 10 days postinoculation, compared to uninoculated controls. These results indicated that PVX and TMV-L11A infection not only affected the quantity, but also altered the type of phenol components of the infected tomato plants (Balogun and Teraoka, 2004). Other studies indicated that increased PAL activity and elevated phenolic contents play active roles in virus defense as verified in resistant cowpea plants infected with $CPSMV_{CE}$ (Varela et al., 2017), *Capsicum baccatum* infected with Pepper yellow mosaic virus (PEPYMV) (Gonçalves et al., 2013), and *Gossypium arboreum* and *Gossypium herbaceum* both infected with Cotton leaf curl burewala virus (CLCuBuV) (Siddique et al., 2014)

Our study showed that the GLU specific activity in $CPSMV_{CE}$-inoculated tobacco leaves was higher than in mock-inoculated controls, at 6 DAI (Fig. 5A). This increase of GLU activity in $CPSMV_{CE}$-inoculated tobacco, may have been induced by the virus as an attempt to degrade deposited callose, a β-1,3-glucan

polysaccharide, at the neck region of plasmodesmata (Zavalievet al., 2013). GLU is an enzyme that degrades callose. Callose accumulation regulates plasmodesmata permeability and limits the cell-to-cell movement of plant viruses, whereas its degradation allows virus spread (Harries and Ding, 2011; Zavaliev et al., 2013; Walsh and and Mohr, 2011). It is well known that viruses subvert the host protein synthesis machinery to their own purpose. The increased GLU activity observed in our study may be an example of such interference on the tobacco protein metabolism.

The cysteine proteinase inhibitor (PIN) of tobacco leaves infected with $CPSMV_{CE}$ was strongly induced at the early stage of infection (Fig. 5B). Plausibly, increased PIN activity constitutes an attempt of tobacco to inhibit the $CPSMV_{CE}$ cysteine proteinase that is required for the proteolytic cleavage of the $CPSMV_{CE}$ RNA 1-encoded polyprotein precursor (208 kDa molecular mass), which is processed to yield five mature, functional protein sub-units (a 32 kDa proteinase cofactor, a 58 kDa presumed helicase, a viral genome 5'-linked protein [VPg] of the CPSMV genomic RNAs [RNA-1 and RNA-2], a 24 kDa proteinase, and a 87 kDa presumed RNA-dependent RNA polymerase) that are required for replication, a crucial event for successful viral infection (Chen and Bruening, 1992; Ponz et al., 1988; Rodamilans et al., 2018). For instance, increased proteinase inhibitor activity was reported in the incompatible interactions of both *G. arboreum* and *G. herbaceum* with CLCuBuV (Siddique et al., 2014) and transgenic tobacco plants infected with Tobacco etch virus (TEV) and Potato virus Y (PTY) (Gutierrez-Campos et al., 1999). Therefore, inhibitors of cysteine proteinases could be further studied as potential antiviral agents against plant viruses that use cysteine proteinases to process genomic precursor proteins for replication.

Viruses depend on the host cellular translation initiation factors to synthesize their proteins to regulate replication, the systemic movement into the plant cells, and complete their cycle (Keima et al., 2017; Sanfaçon, 2015; Shopan et al., 2020; Walsh and Mohr, 2011). The transcript content of the elongation factor *EF1α* (also referred as eEF1A, in the literature) was down-regulated in $CPSMV_{CE}$-inoculated tobacco at 6 DAI, whereas *eIF4E* was up-regulated and its *eIF(iso)4E* isoform did not change. *eIF4E* and *eIF(iso)4E* have similar activities, but may have distinct physiological functions and the lack of eIF4E or eIFiso4E does not influence the viability of plants. However, deficiency of eIF4E or eIFiso4E decreases the infectivity of plant viruses (Keima et al., 2017). For instance, natural recessive resistance to potyvirus and several other viruses has been often linked to mutations in *eIF4E* or *eIF(iso)4E* that impede their interactions with the VPg protein (Sanfaçon, 2015; Shopan et al., 2020). Presumably, $CPSMV_{CE}$ induced the increase of the *eIF4E* gene products (Fig. 6) in tobacco as an attempt to support infection. Therefore, increase of the *EF1α* level was expected, together with *eIF4E*, to enhance the synthesis of the $CPSMV_{CE}$ polyprotein. However, in response to the augmented *eIF4E* expression, the $CPSMV_{CE}$-inoculated tobacco plants down-regulated *EF1α* (Fig. 6). Plausibly, it represents an attempt to control $CPSMV_{CE}$ replication. For instance, $CPSMV_{CE}$ is also a positive-strand RNA virus. *EF1α* is frequently found in association with eIF4E/eIF(iso)4E and PABP (poly(A)-binding protein) to comprise the virus translation/replication complexes of positive-strand RNA viruses (Sanfaçon, 2015). *EF1α* is required to deliver selected aminoacylated tRNA to the 80S ribosome A site (Walsh and Mohr, 2011). The positive-strand RNA virus type constitutes the majority of the characterized infectious plant viruses (Sanfaçon, 2020). Proteomic

analyses of a resistant cowpea genotype infected with $CPSMV_{CE}$ also showed lower *EF1α* accumulation (Varela et al., 2017). Moreover, recent findings by our research group revealed that a susceptible cowpea genotype up-regulated *eIF(iso)4E* when inoculated with $CPSMV_{CE}$, while the resistant cowpea genotype exhibited no alteration in both *eIF4E* and *eIF(iso)4E* (data not published). eIF4E is a major target factor hijacked by *Potyviruses*, to which *Comoviruses* are similar, to enhance protein synthesis, cell-to-cell and systemic movements, and regulate replication (Sanfaçon, 2015).

BRI1 gene, which codes for a receptor kinase, was down-regulated in tobacco plants infected with $CPSMV_{CE}$ as compared to uninoculated controls (Fig. 6). *BRI1* and *BAK1* are receptors for brassinosteroid (BR) signalling and play important functions in infections caused by RNA virus, like those promoted by Turnip crinkle virus (TCV), Oilseed rape mosaic virus (ORMV), and TMV (Zhao and Li, 2021). Silencing of the BR biosynthetic and signaling genes *NbBRI1* and *NbBAK1*, along with *NbDWARF*, *NbBSK1*, and *NbBIK1*, enhanced the susceptibility of *N. benthamiana* plants to TMV infection indicating that these genes also support the antiviral immune response (Deng et al., 2016a). Moreover, silencing of NbBRI1 compromised the BR-induced H_2O_2 and NO production associated with systemic virus resistance (Deng et al., 2016). Therefore, lower *BRI1* expression induced in tobacco by $CPSMV_{CE}$ may represent an additional virus strategy by which the BR-induced resistance of tobacco to $CPSMV_{CE}$ is blocked.

The *NR* gene, which code for nitrite-dependent nitrate reductase, was down-regulated upon tobacco inoculation with $CPSMV_{CE}$ (Fig. 6). Deng et al. (2016) showed that silencing of NbNR or systemic pharmacological inhibition of NR compromised BR-triggered systemic nitric oxide (NO) accumulation that participates in the BR-induced general virus defence signalling in *Nicotiniana benthamiana*. Probably, down-regulation of *NR* in tobacco, induced by $CPSMV_{CE}$, limits the BR-induced defence mechanism of tobacco as there is evidence that H_2O_2 and NO are involved in the BR-mediated systemic defense signaling pathway against plant viruses (Deng et al., 2016; Štolfa Čamagajevac et al., 2019). This suggests that $CPSMV_{CE}$ successfully inhibited the BR-dependent defense pathway in tobacco plants. For instance, BR levels and signalling were positively correlated with the tolerance of *Arabidopsis thaliana* to Cucumber mosaic virus (CMV) (Zhang et al., 2015b). Zou et al. (2018) showed that there is indeed a BR-dependent pathway that induces NO accumulation through NR activity to suppress viral infection in *A. thaliana* challenged with CMV.

We conclude that $CPSMV_{CE}$ modulated the activity of some enzymes and gene expression in tobacco to its own benefit, as proposed in the supplementary Figure S1. Indeed, the genes related to the plant defense pathways (NR, BRI1, and BAK1) had their expression down-regulated, whereas *eIF4E*, which is related to $CPSMV_{CE}$ protein synthesis, replication, and spread, was up-regulated. However, even with alterations induced by $CPSMV_{CE}$ to facilitate the viral action, *N. tabacum* overcomes and actively responds against the viral infection (Fig. S1). For example, the *EF1α* gene, which is also related to viral protein synthesis, was down-regulated. Moreover, the H_2O_2 and polyphenol contents (PC), as well as the activity of the enzymes SOD and PAL increased. Nevertheless, the severe mosaic disease symptoms caused by $CPSMV_{CE}$ in susceptible cowpea genotypes were not developed in *N. tabacum* (var. Xanthi),

although $CPSMV_{CE}$ viral particles were present in the plant leaves at 6 DAI (Fig. 1). Taken together, these findings suggest that *N. tabacum* (var. Xanthi), a non-leguminous plant, exhibited the patterns of a typical tolerant host to $CPSMV_{CE}$ since this virus did not cause any harmful disease symptoms although it modulated some transcripts and enzyme activities crucial for successful viral replication. Nevertheless, other many biochemical and molecular aspects of this pathosystem need to be investigated to obtain a complete picture of the mechanisms driving the tolerance of *N. tabacum* (var. Xanthi) to $CPSMV_{CE,}$ which is of utmost importance to develop new cowpea genotypes tolerant or resistant to this viral disease.

Declarations

Acknowledgments

Authors acknowledge the financial supports from the Council for Advanced Professional Training (CAPES), the Federal University of Ceará, and the National Council for Scientific and Technological Development (CNPq, grant numbers: 308107/2013-6; 431511/2016-0; and 306202/2017-4). R.S.C.B. was supported by CAPES/DS (Proc. 1592074) and is currently supported by CAPES/DS (Proc. 1769099). Y.L-M. was supported by CAPES/DS (Proc. 1280937) and is currently supported by PNPD/CAPES (CAPES/BRASIL, Proc. 88887.473943/2020-00).

Author contribution statement

J.T.A. Oliveira conceived and designed research. R.S.C. Bret, Y. Lima-Melo, and C.P.S. Carvalho conducted the experiments. J.T.A. Oliveira, R.S.C. Bret, Y. Lima-Melo, and C.P.S. Carvalho analyzed the data. J.T.A. Oliveira, R.S.C. Bret, and Y. Lima-Melo wrote the manuscript. All authors read and approved the manuscript.

Funding

This work was financially supported by the Council for Advanced Professional Training (CAPES), Federal University of Ceará-Brazil, and the National Council for Scientific and Technological Development (CNPq, grant numbers: 308107/2013-6; 431511/2016-0; and 306202/2017-4).

Conflict of interest

The authors declare that they have no conflict of interest. The present research did not involve human participants and/or animals. Informed consent was obtained from all individual participants included in the study.

References

1. Abe M, Abe K, Kuroda M, Arai S (1992) Corn Kernel cysteine proteinase inhibitor as a novel cystatin superfamily member of plant origin. Molecular cloning and expression studies. Eur J Biochem

209:933-937. https://doi.org/10.1111/j.1432-1033.1992.tb17365.x

2. Ainsworth EA, Gillespie KM (2007) Estimation of total phenolic content and other oxidation substrates in plant tissues using Folin-Ciocalteu reagent. Nat Protoc 2:875–877. https://doi.org/10.1038/nprot.2007.102
3. Balogun OS, Teraoka T (2004) Time-course analysis of the accumulation of phenols in tomato seedlings infected with *Potato Virus X* and Tobacco mosaic virus. Biokemistri 16:112-120. Doi: 10.4314/biokem.v16i2.32579
4. Boari, AJ, Quadros AFF, Kauffmann CM, Pantoja KFC, Gomes-Junior RA, Freire-Filho FR, Oliveira RP, Cordovil GA, Gavinho BES, Kitajima EW, Blawid R, Nagata T (2021) Near-complete genome sequence of cowpea severe mosaic virus in South America and reduced yardlong bean production due to the viral infection. Trop Plant Pathol 46:487–491 https://doi.org/10.1007/s40858-021-00420-w
5. Boller T (1993) Antimicrobial Functions of the Plant Hydrolases, Chitinase and ß-1,3 Glucanase. In: Fritig F & Legrand M (eds) Mechanisms of plant defense responses, Springer, Dordrecht, pp. 391–400. https://doi.org/10.1007/978-94-011-1737-1_124
6. Bradford MM (1976) A rapid and sensitive method for the for the quantitation of microgram quantities of protein utilizing the principle of protein dye-binding. Anal Biochem 72:248–254. https://doi.org/10.1016/0003-2697(76)90527-3
7. Brioso PST, Santiago LJM, Anjos JRN, Oliveira DE (1996) Identificação de espécies do gênero comovirus através de “polymerase chain reaction”. Fitopatol Bras 21: 219–225
8. Čamagajevac IS, Maronić DS, Pfeiffer TZ, Bek N, Lončarić Z (2019) Nitric oxide and hydrogen peroxide in plant response to biotic stress. In: Gupta D., Palma J., Corpas F. (eds) Nitric oxide and hydrogen peroxide signaling in higher plants. Springer, Cham. pp. 221–243. https://doi.org/10.1007/978-3-030-11129-8_11
9. Caplan JL, Kumar AS, Park E, Padmanabhan MS, Hoban K, Modla S, Czymmek K, Dinesh-Kumar SP (2015) Chloroplast stromules function during innate immunity. Dev Cell 34: 45–57. https://doi.org/10.1016/j.devcel.2015.05.011
10. Chen X, Bruening G (1992) Cloned DNA copies of cowpea severe mosaic virus genomic RNAs: infectious transcripts and complete nucleotide sequence of RNA 1. Virology 191:607-618. https://doi.org/10.1016/0042-6822(92)90236-I
11. Deng XG, Zhu T, Zou LJ, Han XY, Zhou X, Xi DH, Zhang DW, Lin HH (2016) Orchestration of hydrogen peroxide and nitric oxide in brassinosteroid-mediated systemic virus resistance in *Nicotiana benthamiana*. Plant J 85:478–493. https://doi.org/10.1111/tpj.13120
12. Domier LL, Shaw JG, Rhoads RE (1987) Potyviral proteins share amino acid sequence homology with picorna-,como-, and caulimoviral proteins. Virology 158:20–27. Doi: 10.1016/0042-6822(87)90233-9.
13. Garcia-Ruiz H (2019) Host factors against plant viruses. Mol Plant Pathol 20:1588-1601. https://doi.org/10.1111/mpp.12851

14. Garcia-Ruiz H (2018) Susceptibility genes to plant viruses. Viruses 10:484. https://doi.org/10.3390/v10090484
15. Gonçalves LSA, Rodrigues R, Diz MSS, Robaina RR, do Amaral AT, Carvalho AO, Gomes VM (2013) Peroxidase is involved in pepper yellow mosaic virus resistance in *Capsicum baccatum* var. pendulum. Genet Mol Res 12:1411–1420. https://doi.org/10.4238/2013.April.26.3
16. Gutierrez-Campos R, Torres-Acosta JA, Saucedo-Arias LJ, Gomez-Lim MA (1999) The use of cysteine proteinase inhibitors to engineer resistance against potyviruses in transgenic tobacco plants. Nat Biotechnol 17:1223–1226. http://biotech.nature.com
17. Harries P, Ding B (2011) Cellular factors in plant virus movement: At the leading edge of macromolecular trafficking in plants. Virology 411:237–243. https://doi.org/10.1016/j.virol.2010.12.021
18. Havir EA, McHale NA (1987) Biochemical and developmental characterization of multiple forms of catalase in tobacco leaves. Plant Physiol 84:450–455. https://doi.org/10.1104/pp.84.2.450
19. Herrero J, Esteban-Carrasco A, Zapata JM. (2013) Looking for *Arabidopsis thaliana* peroxidases involved in lignin biosynthesis. Plant Physiol Biochem 67:77–86. https://doi.org/10.1016/j.plaphy.2013.02.019
20. Hyodo K, Okuno T (2020) Hijacking of host cellular components as proviral factors by plant-infecting viruses. In: Carr JP & Roossinck MJ (eds) Advances in virus research. Elsevier Inc., pp. 37–86. https://doi.org/10.1016/bs.aivir.2020.04.002
21. Keima T, Hagiwara-Komoda Y, Hashimoto M, Neriya Y, Hiroaki K, Iwabuchi N, Nishida S, Yamaji Y, Namba S (2017) Deficiency of the eIF4E isoform nCBP limits the cell-to-cell movement of a plant virus encoding triple-gene-block proteins in *Arabidopsis thaliana*. Sci Rep 7:39678, Doi: 10.1038/srep39678
22. Kofalvi SA, Nassuth A (1995) Influence of wheat streak mosaic virus infection on phenylpropanoid metabolism and the accumulation of phenolics and lignin in wheat. Physiol Mol Plant Pathol 47:365–377. Doi: 10.1006/pmpp.1995.1065.
23. Koshiba T (1993) Cytosolic ascorbate peroxidase in seedlings and leaves of maize (*Zea mays*). Plant Cell Physiol 34:713–721. https://doi.org/10.1093/oxfordjournals.pcp.a078474
24. Lei R, Du Z, Qiu Y, Zhu S (2016) The detection of hydrogen peroxide involved in plant virus infection by fluorescence spectroscopy. Luminescence 31:1158–1165. Doi: 10.1002/bio.3090.
25. Lima JAA, Kelly A, Aragão L, Ferreira NRA, Teófilo EM (2011) Simple and multiple resistances to viruses in cowpea genotypes, Pesq Agropec Bras 46:1432-1438. http://dx.doi.org/10.1590/S0100-204X2011001100003
26. Livak KJ, Schmittgen TD (2001) Analysis of relative gene expression data using real-time quantitative PCR and the 2-ΔΔCT method. Methods 25:402–408. https://doi.org/10.1006/meth.2001.1262
27. Lomonossoff GP, Ghabrial SA (2001) Comovirus. In: Malloy OC & Murray TD (eds). Encyclopedia of plant pathology, John Wiley and Sons, New York, vol. 1, pp. 239–242.

28. Martins TF, Souza PFN, Alves MS, Silva FDA, Arantes MR, Vasconcelos IM, Oliveira JTA (2020). Identification, characterization, and expression analysis of cowpea (*Vigna unguiculata* [L.] Walp.) miRNAs in response to cowpea severe mosaic virus (CPSMV) challenge. Plant Cell Rep 39:1061–1078. https://doi.org/10.1007/s00299-020-02548-6
29. Medina-Puche L, Lozano-Duran R (2019) Tailoring the cell: a glimpse of how plant viruses manipulate their hosts. Curr Opin Plant Biol https://doi.org/10.1016/j.pbi.2019.09.007
30. Mentel R, Shirrmakher R, Kevich A, Dreĭzin RS, Shmidt I (1977) Virus inactivation by hydrogen peroxide. Vopr Virusol 6:731-733.
31. Murashige T, Skoog F (1962) A revised medium for rapid growth and bio assays with tobacco tissue cultures. Physiol Plant 15:473–497. https://doi.org/10.1111/j.1399-3054.1962.tb08052.x
32. Pagán I, Garcia-Arenal F (2018) Tolerance to plant pathogens: theory and experimental evidence. Int J Mol Sci 19:e810. Doi:10.3390/ijms19030810
33. Paiva ALS, Oliveira JTA, Souza GA, Vasconcelos IM (2016) Label-free proteomics reveals that cowpea severe mosaic virus transiently suppresses the host leaf protein accumulation during the compatible interaction with cowpea (*Vigna unguiculata* [L.] Walp.). J Proteome Res 15:4208–4220. https://doi.org/10.1021/acs.jproteome.6b00211
34. Peixoto PHP, Cambraia J, Sant'Anna R, Mosquim PR, Moreira MA (1999) Aluminum effects on lipid peroxidation and on the activities of enzymes of oxidative metabolism in sorghum. Rev Bras Fisiol Veg 11:137–143.
35. Ponz F, Glascock CB, Bruening G (1988) An inhibitor of polyprotein processing with the characteristics of a natural virus resistance factor. Mol Plant-Microbe Interact 1:25–31. https://www.researchgate.net/publication/250927359
36. Rodamilans B, Shan H, Pasin F, García JA (2018) Plant viral proteases: beyond the role of peptide cutters. Front Plant Sci 9:article 666. https://doi.org/10.3389/fpls.2018.00666
37. Rojas CM, Senthil-Kumar M, Tzin V, Mysore KS (2014) Regulation of primary plant metabolism during plant-pathogen interactions and its contribution to plant defense. Front Plant Sci 5:1–12. https://doi.org/10.3389/fpls.2014.00017
38. Sanfaçon H (2015) Plant translation factors and virus resistance. Viruses 7:3392-3419. https://doi.org/10.3390/v7072778
39. Sanfaçon H (2020) Modulation of disease severity by plant positive-strand RNA viruses: The complex interplay of multifunctional viral proteins, subviral RNAs and virus-associated RNAs with plant signaling pathways and defense responses. Adv Virus Res 107: 87-131. https://doi.org/10.1016/bs.aivir.2020.04.003
40. Stephenie S, Chang YP, Gnanasekaran A, Esa NM, Gnanaraj C (2020) An insight on superoxide dismutase (SOD) from plants for mammalian health enhancement. J Funct Foods 68:103917. Doi: 10.1016/j.jff.2020.103917
41. Sharma P, Jha AB, Dubey RS, Pessarakli M (2012) Reactive oxygen species, oxidative damage, and antioxidative defense mechanism in plants under stressful conditions. J Bot 2012, article 217037.

https://doi.org/10.1155/2012/217037

42. Shopan J, Lv X, Hu Z, Zhang M, Yang J (2020) Eukaryotic translation initiation factors shape RNA viruses resistance in plants. Hortic Plant J 6:81-88. https://doi.org/10.1016/j.hpj.2020.03.001
43. Siddique Z, Akhtar KP, Hameed A, Sarwar N, Imran-Ul-Haq, Khan S.A., 2014. Biochemical alterations in leaves of resistant and susceptible cotton genotypes infected systemically by cotton leaf curl Burewala virus. J Plant Interact 9:702–711. https://doi.org/10.1080/17429145.2014.905800
44. Silva RGG, Vasconcelos IM, Martins TF, Varela ALN, Souza PFN, Lobo AKM, Silva FDA, Silveira JAG, Oliveira JTA (2016) Drought increases cowpea (*Vigna unguiculata* [L.] Walp.) susceptibility to cowpea severe mosaic virus (CPSMV) at early stage of infection. Plant Physiol Biochem 109:91–102. https://doi.org/10.1016/j.plaphy.2016.09.010
45. Smirnoff N., Arnaud D (2019) Hydrogen peroxide metabolism and functions in plants. New Phytol 221:1197-1214. Doi: 10.1111/nph.15488
46. Souza PFN, Silva FDA, Carvalho FEL, Silveira JAG, Vasconcelos IM, Oliveira JTA (2017) Photosynthetic and biochemical mechanisms of an EMS-mutagenized cowpea associated with its resistance to cowpea severe mosaic virus. Plant Cell Rep 36:219–234. https://doi.org/10.1007/s00299-016-2074-z
47. Thordal-Christensen H, Zhang Z, Wei Y, Collinge DB (1997) Subcellular localization of H_2O_2 in plants. H_2O_2 accumulation in papillae and hypersensitive response during the barley-powdery mildew interaction. Plant J 11:1187–1194. https://doi.org/10.1046/j.1365-313X.1997.11061187.x
48. Underwood W (2012) The plant cell wall: a dynamic barrier against pathogen invasion. Front Plant Sci 3:1–6. https://doi.org/10.3389/fpls.2012.00085
49. Urbanek H, Kuzniak-Gebarowska E, Herka H (1991) Elicitation of defense responses in bean leaves by *Botrytis cinerea* polygalacturonase. Acta Physiol Plant 13, 43-50.
50. van Rossum MWP, Alberda M, van der Plas LH (1997) Role of oxidative damage in tulip bulb scale micropropagation. Plant Sci 130:207–216. https://doi.org/10.1016/S0168-9452(97)00215-X
51. Varela ALN, Komatsu S, Wang X, Silva RGG, Souza PFN, Lobo AKM, Vasconcelos IM, Silveira JAG, Oliveira JTA (2017) Gel-free/label-free proteomic, photosynthetic, and biochemical analysis of cowpea (*Vigna unguiculata* [L.] Walp.) resistance against Cowpea severe mosaic virus (CPSMV). J Proteomics 163:76–91. https://doi.org/10.1016/j.jprot.2017.05.003
52. Walsh D, Mohr I (2011) Viral subversion of the host protein synthesis machinery. Nat Rev Microbiol 9: 860–875. Doi:10.1038/nrmicro2655
53. Weber PH, Bujarski JJ (2015) Multiple functions of capsid proteins in (+) stranded RNA viruses during plant-virus interactions. Virus Res 196:140–149. https://doi.org/10.1016/j.virusres.2014.11.014
54. Yang H, Wang M, Gao Z, Zhu C, Guo X (2011) Isolation of a novel RNA-dependent RNA polymerase 6 from *Nicotiana glutinosa*, NgRDR6, and analysis of its response to biotic and abiotic stresses. Mol Biol Rep 38:929–937. https://doi.org/10.1007/s11033-010-0186-z

55. Zaulda FA, Zhang S, Han J, Qu F (2019). Generation of a Cowpea Severe Mosaic Virus Infectious Clone. APS Annual Meeting, Cleveland, Ohio, USA (3-7 august, 2019).
56. Zavaliev R, Levy A, Gera A, Epel BL (2013) Subcellular dynamics and role of Arabidopsis β-1,3-glucanases in cell-to-cell movement of tobamoviruses. Mol Plant Microbe Interact 26:1016–1030. https://doi.org/10.1094/MPMI-03-13-0062-R
57. Zhang C, Wu Z, Li Y, Wu J (2015a) Biogenesis, function, and applications of virus-derived small RNAs in plants. Front Microbiol 6:1–12. https://doi.org/10.3389/fmicb.2015.01237
58. Zhang DW, Deng XG, Fu FQ, Lin HH (2015B) Induction of plant virus defense response by brassinosteroids and brassinosteroid signaling in *Arabidopsis thaliana*. Planta 241:875–85. https://doi.org/10. 1007/s00425-014-2218-8
59. Zhang X-N, Liao Y-W-K, Wang X-R, Zhang L, Ahammed GJ, Li Q-Y, Li X (2020) Epigallocatechin-3-gallate enhances tomato resistance to tobacco mosaic virus by modulating RBOH1-dependent H_2O_2 signaling. Plant Physiol Biochem 150:263–269. https://doi.org/10.1016/j.plaphy.2020.03.008
60. Zhao S, Li Y (2021) Current understanding of the interplays between host hormones and plant viral infections. PLoS Pathog 17:e1009242. https://doi.org/10.1371/journal.ppat.1009242
61. Zhou M, Diwu Z, Panchuk-Voloshina N, Haugland RP (1997) A stable nonfluorescent derivative of resorufin for the fluorometric determination of trace hydrogen peroxide: Applications in detecting the activity of phagocyte NADPH oxidase and other oxidases. Anal Biochem 253:162–168. https://doi.org/10.1006/abio.1997.2391
62. Zou L-J, Deng X-G, Zhang L, Zhu T, Tan W-R, Muhammad A, Zhu L-J, Zhang C, Zhang D-W, Lin H-H (2018) Nitric oxide as a signaling molecule in brassinosteroid-mediated virus resistance to Cucumber mosaic virus in *Arabidopsis thaliana*. Physiol Plant 163:196–210. https://doi.org/10.1111/ppl.12677

Figures

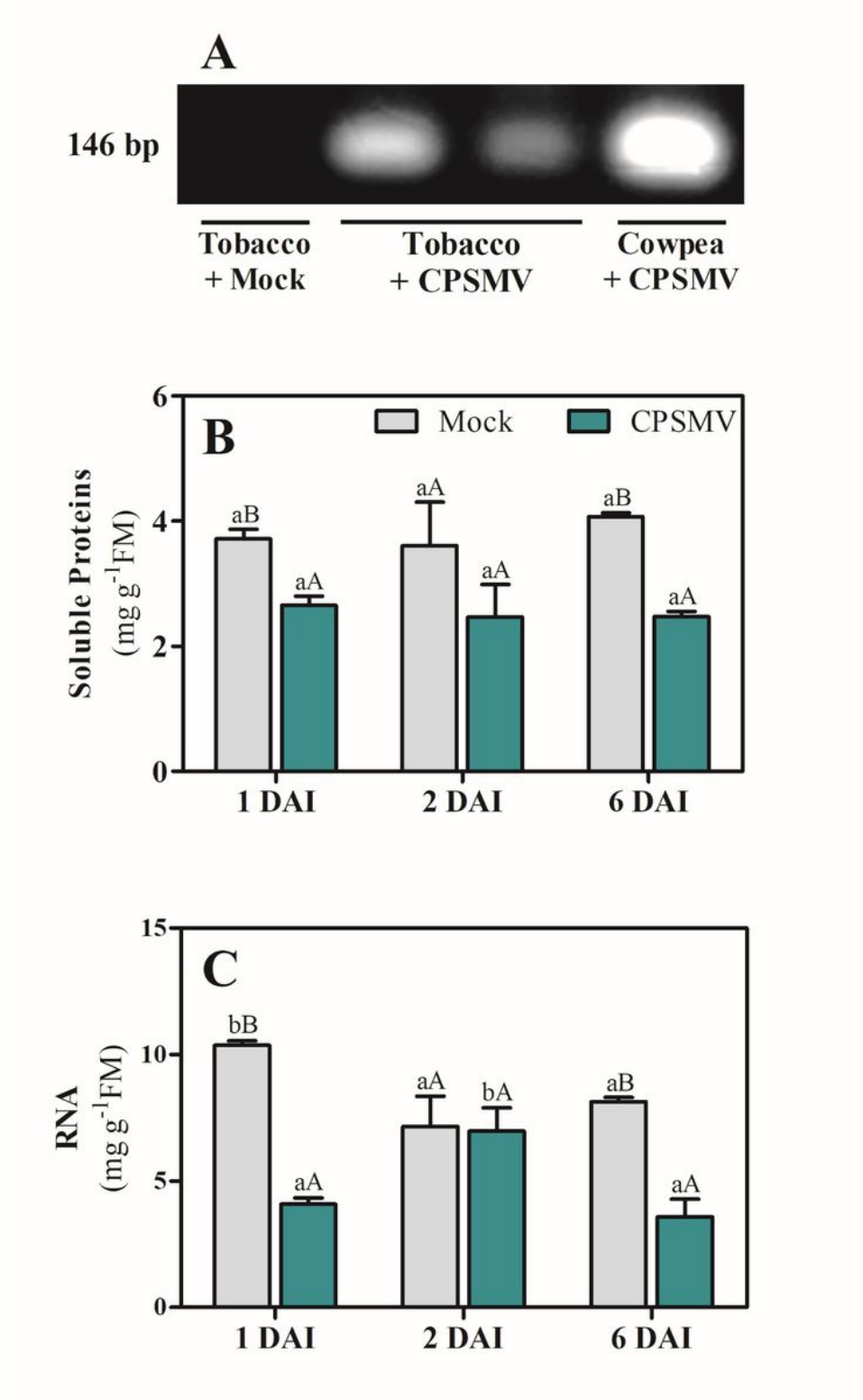

Figure 1

PCR products (cDNA) of the CPSMV coat protein (A), and the contents of the leaf protein (B) and RNA (C) of tobacco plants. The mock- (Tobacco + Mock) control and the CPSMV-inoculated (Tobacco + CPSMV) tobacco leaves were analyzed. For comparison, a susceptible cowpea genotype (CE-31), equally inoculated with CPSMV (Cowpea + CPSMV), was included. The PCR products (cDNA) of the CPSMV coat protein were assessed at 6 days after CPSMV inoculation (6 DAI) by electrophoresis in 1.5% (v/v) agarose

gel. The leaf soluble protein and RNA contents were evaluated in mock- (mock) and CPSMV-inoculated (CPSMV) tobacco leaves at 1, 2, and 6 DAI. Each time point represents the mean of three independent samples with three analytical replicates each ± standard deviation. Different lower-case letters indicate significant ($p \leq 0.05$) difference between the means of the same treatment plant group along the experimental days (1 DAI, 2 DAI, and 6 DAI), according to the analysis of variance (ANOVA) followed by the Tukey's test. Different upper-case letters indicate significant ($p \leq 0.05$) difference between the means of the two treatment groups (mock- and CPSMV-inoculated plants) compared at each time point.

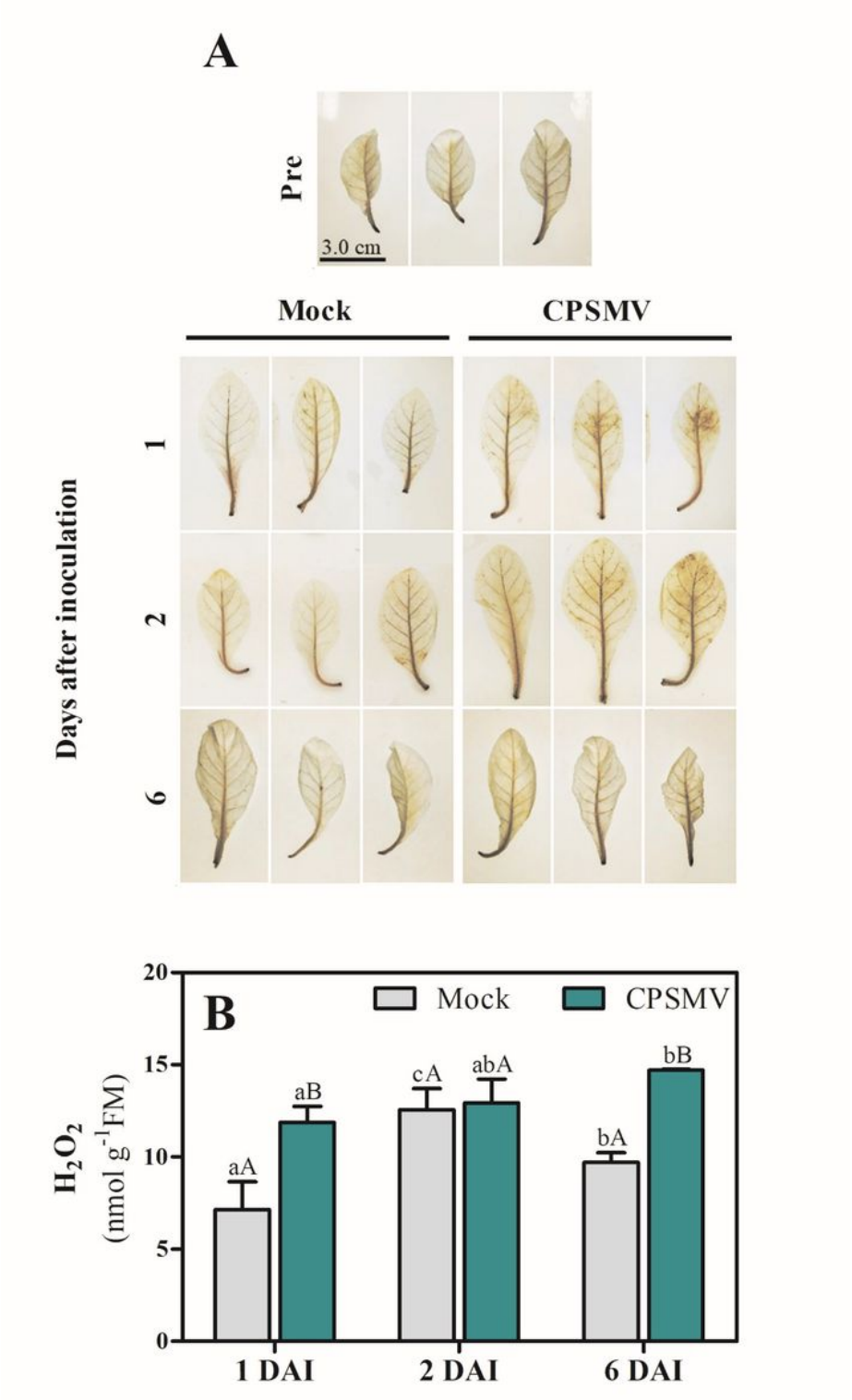

Figure 2

In situ H_2O_2 accumulation (A) and H_2O_2 content (B) in CPSMV-inoculated tobacco leaves measured at 1, 2, and 6 days after CPSMV inoculation (DAI) compared with the respective mock-inoculated controls. Each leaf represents an independent biological sample. Each data point represents the mean of three independent samples with three analytical replicates each ± standard deviation. Different lower-case letters indicate significant ($p \leq 0.05$) difference between the means of the same treatment plant group along the experimental days (1 DAI, 2 DAI, and 6 DAI), according to the analysis of variance (ANOVA) followed by the Tukey's test. Different upper-case letters indicate significant ($p \leq 0.05$) difference between the means of the two treatment groups (mock- and CPSMV-inoculated plants) compared at each time point.

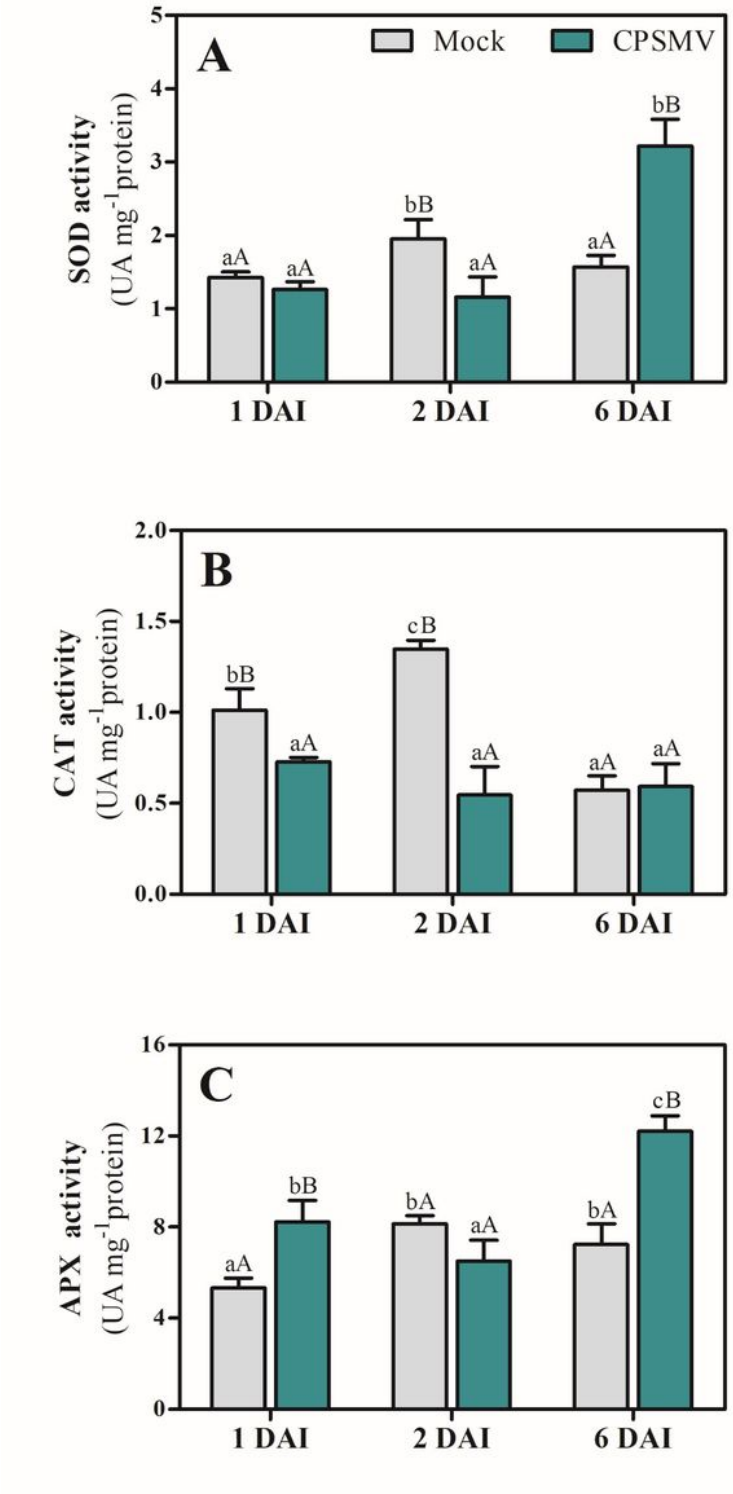

Figure 3

Superoxide dismutase (SOD; A), catalase (CAT; B), and ascorbate peroxidase (APX; C) enzyme activity at 1, 2, and 6 days after CPSMV inoculation (DAI) compared with the respective mock-inoculated controls. Each data point represents the mean of three independent samples with three analytical replicates each ± standard deviation. Different lower-case letters indicate significant ($p \leq 0.05$) difference between the means of the same treatment plant group along the experimental days (1 DAI, 2 DAI, and 6 DAI),

according to the analysis of variance (ANOVA) followed by the Tukey's test. Different upper-case letters indicate significant ($p \leq 0.05$) difference between the means of the two treatment groups (mock- and CPSMV-inoculated plants) compared at each time point.

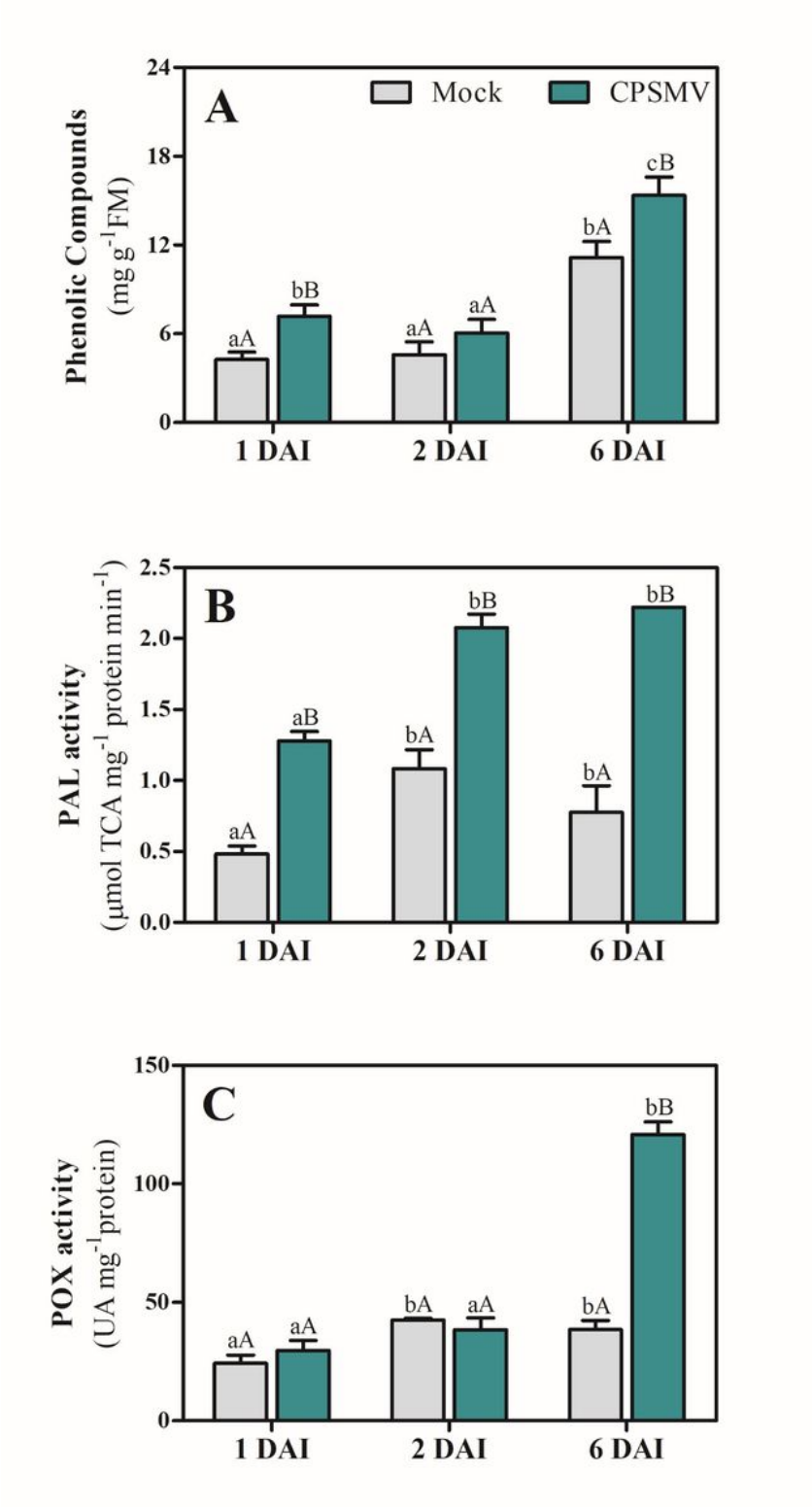

Figure 4

Phenolic compound content (PC; A) and activities of phenylalanine ammonia-lyase (PAL; B) and guaiacol peroxidase (POX; C) at 1, 2, and 6 days after CPSMV inoculation (DAI) compared with the respective mock-inoculated controls. Each data point represents the mean of three independent samples with three analytical replicates each ± standard deviation. Different lower-case letters indicate significant ($p \leq 0.05$) difference between the means of the same treatment plant group along the experimental days (1 DAI, 2 DAI, and 6 DAI), according to the analysis of variance (ANOVA) followed by the Tukey's test. Different upper-case letters indicate significant ($p \leq 0.05$) difference between the means of the two treatment groups (mock- and CPSMV-inoculated plants) compared at each time point.

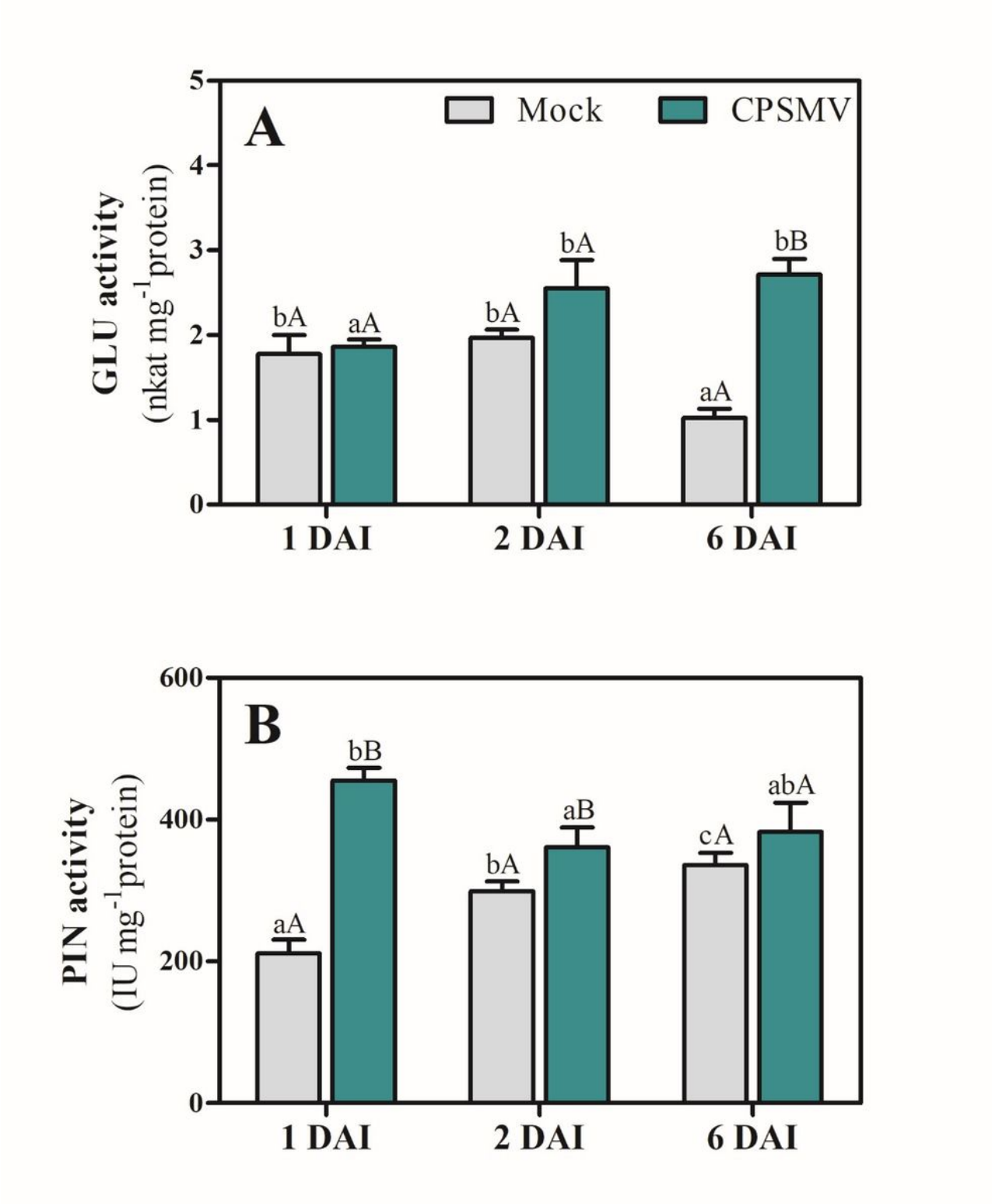

Figure 5

β-1,3-glucanase (GLU; A) and papain inhibitor (PIN; B) activities at 1, 2, and 6 days after CPSMV inoculation (DAI) compared with the respective mock-inoculated controls. Each data point represents the mean of three independent samples with three analytical replicates each ± standard deviation. Different lower-case letters indicate significant ($p \leq 0.05$) difference between the means of the same treatment plant group along the experimental days (1 DAI, 2 DAI, and 6 DAI), according to the analysis of variance

(ANOVA) followed by the Tukey's test. Different upper-case letters indicate significant ($p \leq 0.05$) difference between the means of the two treatment groups (mock- and CPSMV-inoculated plants) compared at each time point.

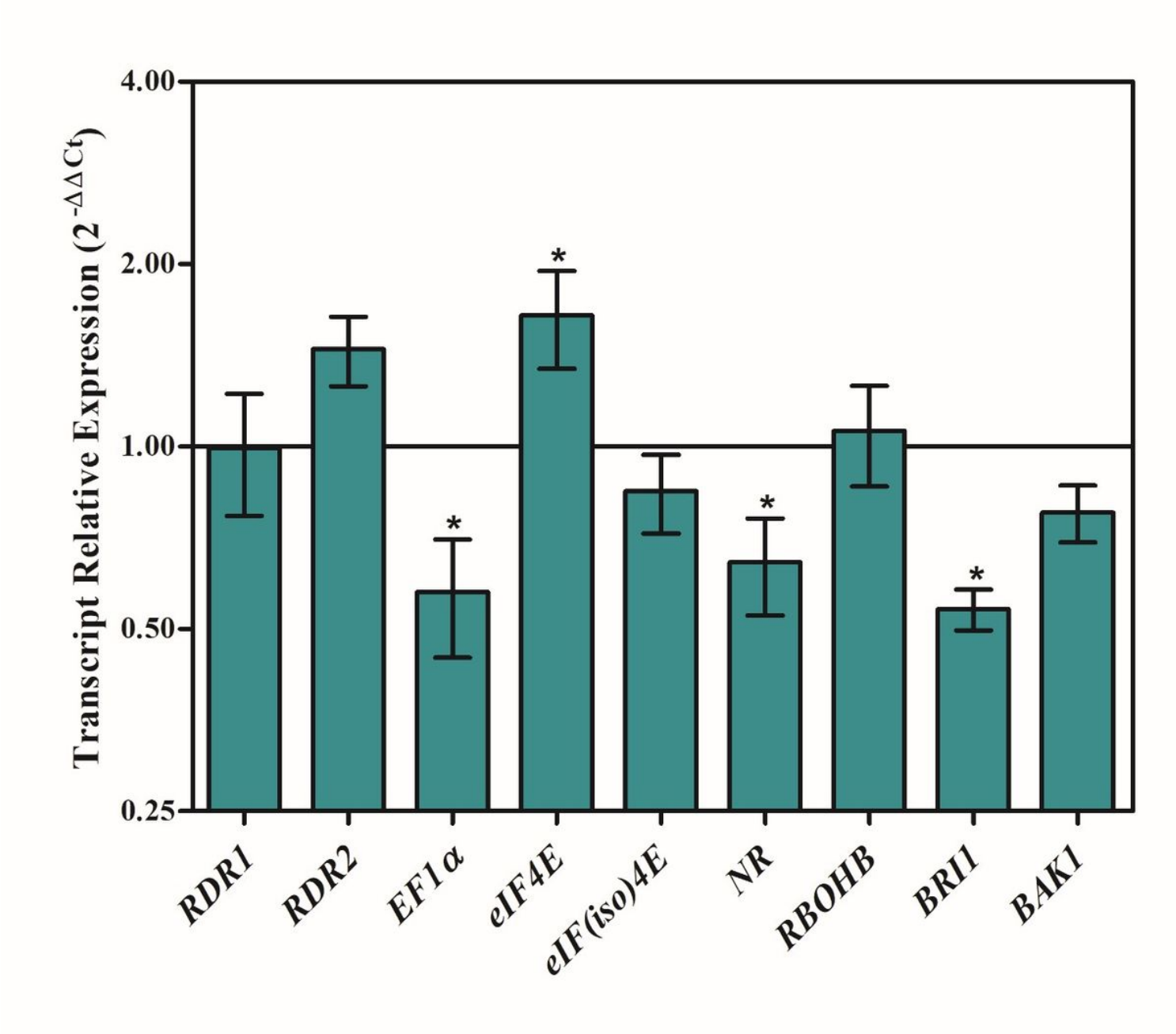

Figure 6

Relative transcript levels of RNA-dependent RNA polymerase 1 (*RDR1*), RNA-dependent RNA polymerase 2 (*RDR2*), elongation factor 1α (*EF1α*), eukaryotic translation initiation factor 4E (*eIF4E*), eukaryotic translation initiation factor isoform 4E (*eIF(iso)4E*), nitrate reductase (*NR*), respiratory burst oxidase homolog protein B (*RBOHB*), brassinosteroid insensitive 1-associated receptor kinase 1 (*BAK1*), and brassinosteroid insensitive 1 (*BRI1*) in CPSMV-inoculated tobacco leaves at 6 days after CPSMV inoculation (6 DAI). The values are relative to the transcript expression values in the mock-inoculated

leaves also at 6 DAI. Each data point represents the mean of three independent samples with three analytical replicates each ± standard deviation. Asterisks indicate significant ($p \leq 0.05$) difference between treatments (mock- and CPSMV-inoculated plants) as evaluated by the Student's Test.

Supplementary Files

This is a list of supplementary files associated with this preprint. Click to download.

- FigureS1.tif.docx